A LETTERS JOURNAL EXPLORING THE FRONTIERS OF PHYSICS

OFFPRINT

The generation of Parkinsonian tremor as revealed by directional coupling analysis

D. A. Smirnov, U. B. Barnikol, T. T. Barnikol, B. P. Bezruchko, C. Hauptmann, C. Bührle, M. Maarouf, V. Sturm, H.-J. Freund and P. A. Tass

EPL, **83** (2008) 20003

TAKE A LOOK AT THE NEW EPL

Europhysics Letters (EPL) has a new online home at
www.epljournal.org

Take a look for the latest journal news and information on:

- reading the latest articles, free!
- receiving free e-mail alerts
- submitting your work to EPL

www.epljournal.org

A Letters Journal Exploring the Frontiers of Physics

July 2008

EPL, **83** (2008) 20003 www.epljournal.org
doi: 10.1209/0295-5075/83/20003

The generation of Parkinsonian tremor as revealed by directional coupling analysis

D. A. Smirnov[1,2(a)], U. B. Barnikol[1,3,4], T. T. Barnikol[1], B. P. Bezruchko[1,2], C. Hauptmann[1], C. Bührle[1,3,4], M. Maarouf[1,3,4], V. Sturm[3], H.-J. Freund[1,3,4] and P. A. Tass[1,3,4]

[1] *Institute of Neuroscience and Biophysics 3 - Medicine and Virtual Institute of Neuromodulation, Research Center Jülich - D-52425, Jülich, Germany, EU*
[2] *Saratov Branch of the Institute of RadioEngineering and Electronics of the Russian Academy of Sciences 38 Zelyonaya St., Saratov 410019, Russia*
[3] *Department of Stereotaxic and Functional Neurosurgery, University of Cologne - D-50924 Cologne, Germany, EU*
[4] *Brain Imaging Center West - D-52425 Jülich, Germany, EU*

received 27 February 2008; accepted in final form 6 June 2008
published online 10 July 2008

PACS 05.45.Xt – Synchronization; coupled oscillators
PACS 05.45.Tp – Time series analysis
PACS 87.19.xp – Motor system disease (Parkinson's, etc.)

Abstract – To reveal the dynamic mechanism underlying Parkinsonian resting tremor, we applied a phase dynamics modelling technique to local field potentials and accelerometer signals recorded in three Parkinsonian patients with implanted depth electrodes. We detect a bidirectional coupling between the subcortical oscillation and the tremor. The tremor→brain driving is a linear effect with a small delay corresponding to the neural transmission time. In contrast, the brain→tremor driving is a nonlinear effect with a long delay in the order of 1–2 mean tremor periods. Our results are well reproduced for an ensemble of 41 tremor epochs in three Parkinsonian patients and confirmed by surrogate data tests and model simulations. The uncovered mechanism of tremor generation suggests to specifically counteract tremor by desynchronizing the subcortical oscillatory neural activity.

Introduction. – Synchronization is a generic phenomenon which has been studied in different fields of the natural sciences [1]. To understand the mechanisms behind synchronization processes, different techniques have been developed to detect the directionality of the coupling of oscillators [2–11]. Some of these methods have, *e.g.*, been applied to cardiorespiratory interaction [12].

Another challenging issue is tremor generation in Parkinson's disease. In patients with Parkinsonian resting tremor populations of neurons located in the thalamus and basal ganglia fire in a synchronized and periodical manner at a frequency similar to that of the tremor [13]. In contrast, under physiological (healthy) conditions these neurons fire incoherently [14]. But there is an important peripheral mechanism involved in the generation of these abnormal oscillations: the receptor properties in the muscle spindles. They contribute to a servo control (closed-loop control of position and velocity) and amplify the synchronized input from central nervous structures by strongly synchronized feedback [15]. The resulting servo loop oscillations are regarded as a basic mechanism for tremor generation [15]. A closer analysis of these mutual interdependences showed that the subcortical oscillations are not strictly correlated with tremor [16]. As yet, there is no firm evidence to support the hypothesis that the tremor is driven by the subcortical oscillations [16,17]. With linear data analysis tools it has been shown that the tremor drives the subcortical oscillations by the proprioceptive feedback from muscle spindles [18,19].

Here, we set out to use the "phase coherence" of tremor (*i.e.* the high stability of the instantaneous period of the tremor oscillation) to analyze the coupling from the phase dynamics of the oscillations with a recently developed technique [2,5], which is the most sensitive one for phase coherent systems [20,21], in combination with established surrogate analysis. We show that the subcortical oscillations, in fact, drive the tremor. Furthermore, we disentangle the directional coupling characteristics between tremor and subcortical oscillations, the corresponding delays as well as the type of driving effect (linear tremor→brain *vs.* nonlinear brain→tremor influence).

(a) E-mail: smirnovda@yandex.ru

Data description. – In three Parkinson's disease (PD) patients with predominant resting tremor we simultaneously recorded the local field potential (LFP) from the subthalamic nucleus (STN) (patients # 1 and 3) or the ventrointermediate nucleus (VIM) (patient # 2) of the thalamus and the accelerometer signal assessing the hand tremor (fig. 1). Recordings were performed during or after deep brain stimulation (DBS) electrode implantation. *Patient # 1:* Tremor of the left arm more pronounced than on the right. Intraoperative recording from the right STN with the ISIS MER system (Inomed, Teningen, Germany). *Patient # 2:* Tremor of the right arm. Intraoperative recording from the left VIM with the ISIS MER system. *Patient # 3:* Tremor of both arms. Postoperative recording from DBS lead 3387 (Medtronic, Minneapolis) in left STN. LFP was measured between tip macro-contact (in the target) and uppermost contact (reference). Proper electrode placement was confirmed by effective high-frequency macro-stimulations, intraoperative X-ray controls [22], postoperative CT scans, and intraoperative micro-recordings (in patients # 1 and 2). Patients # 1 and 3 had a bilateral tremor, and patient # 2 a unilateral tremor. The study was approved by the local ethical committee. Patients gave their written consent.

During epochs of high-amplitude resting tremor accelerometer signals exhibit a sharp peak in the power spectrum (fig. 1(c)), usually reflected in the LFP recorded from the depth electrode contralateral to (*i.e.*, at the opposite side of) the tremor (fig. 1(d)) (see [16,17]). Typically, tremor is highly regular or "phase coherent", as revealed, *e.g.* by calculating the coefficient of variation k of the instantaneous oscillation period. We obtain its rough estimate from the accelerometer signal bandpass filtered around the tremor frequency (*e.g.*, from 2–6 Hz in fig. 1(c)): $k = \langle T_i \rangle^{-1} \sqrt{\langle (T_i - \langle T_i \rangle)^2 \rangle}$, where the angular brackets denote averaging over time, and T_i are the intervals between successive maxima of the signal. We obtain k typically in the range of 0.01–0.4, predominantly 0.05–0.1. For such data the directionality analysis applied to the phase dynamics is most appropriate [20]. Magnetoencephalographical recordings have shown that the phases (rather than amplitudes) of cerebral and tremor activity are synchronized in PD patients [23].

Coupling estimation technique. – To detect coupling between accelerometer and LFP signal, denoted as $x_1(t)$ and $x_2(t)$, we used several techniques including the traditional cross-correlation function (CCF). We also calculated the time-shifted phase synchronization index [3,24] between the signals: $\rho(\Delta) = |\langle \exp(j(\phi_1(t) - \phi_2(t + \Delta)))\rangle|$, where the angle brackets denote temporal averaging[1]. For this, we first performed a bandpass filtering of $x_1(t)$ and $x_2(t)$ around the tremor frequency (*e.g.* 2–6 Hz in fig. 1(e), (f)) and extracted the phases $\phi_1(t)$, $\phi_2(t)$ with the Hilbert transform [27]. Our results are stable against considerable variations of the band edges and hardly change if the lower cut-off frequency lies between 2 Hz (to filter out low-frequency components of the LFP) and $f_T - 1$ Hz, where f_T is the tremor frequency. The higher cut-off frequency should be between $f_T + 1$ Hz and $2f_T - 1$ Hz.

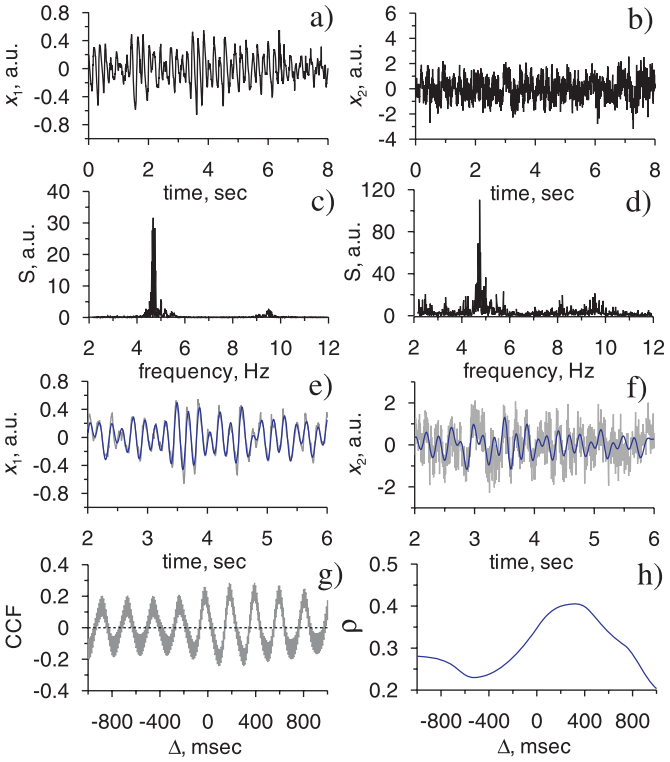

Fig. 1: A spontaneous epoch of Parkinsonian resting tremor in patient #1. a) Accelerometer signal, at the beginning of an 83.5 s long epoch. b) Simultaneous LFP signal. c), d) Power spectra of accelerometer and LFP signals. e), f) Magnified segments of original (grey lines) and bandpass-filtered (blue lines, frequency band 2–6 Hz) signals. g) CCF between accelerometer and LFP signals with 95% confidence bands estimated via Bartlett's formula. h) Phase synchronization index for the phases defined in the frequency band 2–6 Hz.

To reveal the directional coupling, we used the phase dynamics modelling technique which is, in essence, the Granger causality [28] applied to the phases of oscillations [2]. As a model we use coupled phase oscillators:

$$\phi_j(t+\tau) - \phi_j(t) = F_j[\phi_j(t), \phi_k(t-\Delta_j), a_j] + \varepsilon_j(t), \quad (1)$$

where $j, k = 1, 2$ ($j \neq k$), and τ is a fixed time interval equal to the basic period of oscillations, $\varepsilon_k(t)$ are zero-mean noises, F_k trigonometric polynomials of third order [2,5], a_j are vectors of their coefficients, Δ_j are trial time delays [3]. At each Δ_j the estimates of a_j are obtained via the least-squares routine, *i.e.* by searching for the minimal mean squared error $\sigma_j^2(\Delta_j) = \min_{a_j} \langle \{\phi_j(t+\tau) - \phi_j(t) - F_j[\phi_j(t), \phi_k(t-\Delta_j), a_j]\}^2 \rangle$. Thereby, we get the estimate $\hat{a}_j(\Delta_j)$, *i.e.* the model function $F_j(\phi_j, \phi_k, \hat{a}_j)$ for each Δ_j. Coupling strength and time delay estimates are found from the dependence $\hat{a}_j(\Delta_j)$ according to the following idea.

[1]Similar indices were used to study phase synchronization i) between Parkinsonian tremor of both hands [25] and ii) between both legs during Parkinsonian gait [26].

If the "true" equations for the phase dynamics including the "true" coefficients $a_{j,\mathrm{true}}$ were known *a priori*, then the "strengths" c_1 and c_2 of the influences $2\to1$ and $1\to2$ could be defined as $c_j^2=\frac{1}{2\pi^2}\times\int_0^{2\pi}\int_0^{2\pi}\left(\partial F_j(\phi_j,\phi_k,a_{j,\mathrm{true}})/\partial\phi_k\right)^2\mathrm{d}\phi_1\,\mathrm{d}\phi_2$ [2,5] (see footnote [2]). The estimators γ_j for c_j^2, expressed via the estimates $\hat{a}_j$, provide 95% confidence bands, which read $(\gamma_j-1.6\sigma_{\gamma_j},\gamma_j+1.8\sigma_{\gamma_j})$, where the standard deviations σ_{γ_j} are calculated from the same time series [5]. Since γ_j are unbiased estimates of c_j^2 under mild conditions, they can be negative although $c_j^2>0$. Only positive values of γ_j can indicate the presence of coupling. The presence of the influence $k\to j$ follows from $\gamma_j(\Delta_j)-1.6\sigma_{\gamma_j}(\Delta_j)>0$ for a range of trial delays Δ_j of at least half a basic period and requires i) the phase synchronization ρ of the corresponding delays to be moderate (*i.e.* below approximately 0.5), and ii) the time series not to be shorter than 30–50 periods [6,7]. The location of the maximum of $\gamma_j(\Delta_j)$ provides an estimate of the time delay[3]. The corresponding values σ_j^2 are the noise intensities in eqs. (1) and quantify the irregularity of the oscillation period in both processes.

We checked the statistical significance of the results in four ways: We used analytical confidence intervals for γ_k [5] (first test). The test rejects the null hypothesis of uncoupled phase oscillators if $\gamma_k-1.6\sigma_{\gamma_k}>0$. We compared the estimation results for the observed data with two different kinds of surrogate data: we used surrogates preserving only individual power spectra, AAFT surrogates [29], (second test) and Fourier coherence preserving surrogates [30] (third test). The second test checks against the null hypothesis of independent AR processes. The third test checks against the null hypothesis of linearly coupled AR processes (*e.g.* caused by signal mixing due to superposition). Since mixing of the accelerometer and LFP signals is not possible due to their remote origins and recording sites, the last test provides an additional characterization of the coupling in terms of its linearity or nonlinearity. Finally, we compare the observed results with the estimates obtained from simulated time series of a simple model of coupled oscillators which reproduces the noise levels σ_j^2 of the experimental signals. This enables us to assess the time resolution of our approach to the delay time estimation (fourth test).

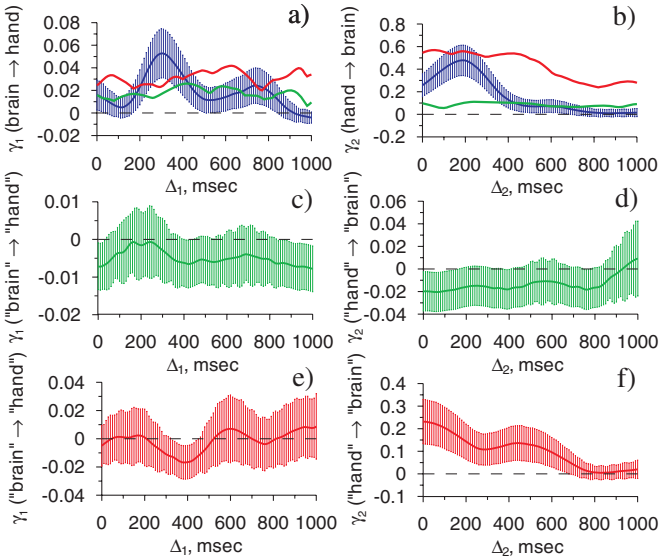

Fig. 2: Coupling characteristics of the epoch shown in fig. 1 *vs.* trial time delay. Error bars denote analytically estimated 95% confidence bands. a) Estimated brain→tremor influence (blue line with error bars), maximal value of 99 AAFT surrogates (green line), maximum over 99 coherence preserving surrogates (red line). b) Estimated tremor→brain influence. c), d) The same plots for a single pair of AAFT surrogate signals preserving only individual power spectra. e), f) The same plots for a single pair of coherence preserving surrogates. Inverted commas ("brain", "hand") refer to surrogates.

Single-epoch analysis. – Figure 1 illustrates the significant interdependence between LFP and contralateral hand during a single typical tremor epoch from patient #1: Within a range of time lags the CCF, together with its 95% confidence bands (grey curve), differs from zero (fig. 1(g)). Phase synchronization achieves a maximum of $\rho=0.41$ at $\Delta=325\,\mathrm{ms}$ (fig. 1(h)), which is not too high, so that the phase dynamics modelling technique is applicable. The latter reveals a significant influence in both directions (fig. 2(a), (b)) as shown by the analytical confidence intervals. The contralateral hand→brain influence is very pronounced: $\gamma_2(0)=0.26$. Despite the maximum at $\Delta_2=185\,\mathrm{ms}$, the value of $\gamma_2(185)$ differs from $\gamma_2(0)$ only within the confidence bands and, hence, it is not possible to infer that the time delay is significantly different from 0. As we show below, according to the average estimates the time delay is at most several dozens of milliseconds. The brain→tremor influence is also highly significant: $\gamma_1(305)=0.05$. The time delay $\Delta_1=305\,\mathrm{ms}$ is more pronounced and stable for this direction.

For an ensemble of 99 power spectrum preserving surrogates, the characteristics $\gamma_{1,2}$ are not different from zero in terms of the above analytical confidence interval in the entire range of trial time delays (fig. 2(c), (d)). The maximal values over the 99 surrogates are indicated by the dashed line in fig. 2(a), (b). The peak values of

[2]To assess the coupling strength, we compare c_j to the mean phase increment $\phi_j(t+\tau)-\phi_j(t)\approx2\pi$ ($\tau\approx$ a mean period). For weak coupling ($c_j\ll2\pi$) the contribution of the coupling terms to the phase increment is much smaller than the contribution of the basic frequency term.

[3]A small τ in eq. (1) (one sampling interval) is good for an accurate time delay Δ_j estimation [3]. But the analytic confidence bands for γ_j [5] are reliable only if the low-order polynomials used capture the phase dynamics. This may be violated for small τ (*i.e.* "fast" phase dynamics) and lead to a spurious coupling detection. Here, we preferred to ensure higher reliability of the coupling detection ($\tau\approx$ a mean period) at the cost of possibly lower accuracy in the Δ_j estimation. Δ_j can also be estimated by minimizing the model error $\sigma_j^2(\Delta_j)$ [3]. γ_j is approximately a weighted sum of squared coefficients $\hat{a}_j(\Delta_j)$. An increase of the coefficients $\hat{a}_j$ minimizes σ_j^2 and maximizes γ_j. In our data maxima of $\gamma_j(\Delta_j)$ and minima of $\sigma_j^2(\Delta_j)$ nearly coincided.

$\gamma_{1,2}$ in fig. 2(a), (b) obtained from the real data are three times greater, *i.e.* according to AAFT surrogate testing $\gamma_{1,2}$ are significant as well, at least, at the significance level $p < 0.01$. Therefore, the results of the coupling estimation are not due to the signals' spectral properties, especially the bandpass chosen for the phase calculation.

For the coherence preserving surrogates typical coupling characteristics are shown in fig. 2(e), (f). One observes almost the same plots for the tremor→brain influence as observed from the real data, indicating that it is a linear effect. Figure 2(f) is similar to fig. 2(b) in the sense that γ_2 is statistically significantly greater than zero for zero time delay. Furthermore, $\gamma_2(\Delta_2)$ is not significantly greater than $\gamma_2(0)$ for any trial time delay Δ_2. A backward influence is not observed in the surrogate time series. Thus, the phase dynamics analysis is sensitive, whereas a usual linear autoregressive modelling underlying coherence preserving surrogates would not detect the brain→tremor influence (fig. 2(e)). The results are confirmed with an ensemble of surrogate data, see red lines in fig. 2(a), (b).

Ensembles of tremor epochs. – In all patients epochs with tremor occurred intermittently. For short epochs the results of our estimation of the curves $\gamma_j(\Delta_j)$ are strongly fluctuating. This is likely to be interpreted as an effect of noise, which can be reduced by using epochs of sufficient length. To reveal reliable coupling estimates with the phase dynamics modelling, we had to select tremor epochs of sufficient length. Tremor epochs of a length not shorter than 70 basic periods turned out to give reproducible results. Figure 1 shows one of the longest epochs, consisting of 418 periods. This interval is characterized by a reliable and typical directionality pattern (fig. 2), which was reproduced in 10 out of 12 epochs in patient #1, in 10 out of 14 epochs in patient #2 and in 10 out of 15 epochs in patient #3, *i.e.* in about 75% of the tremor epochs. In the other 25% of epochs, significant directional coupling was not detected and, typically, cross-correlation was also insignificant.

For every patient, we selected only artifact-free epochs with pronounced tremor (amplitude approximately 5 times greater than "background activity") and averaged the directionality results across them (fig. 3). In this way for all three patients we obtained consistent results, confirming the coupling pattern from fig. 2: we revealed a bi-directional coupling at time delays close to 0 for the contralateral hand→brain direction and a delay of about 1–2 mean periods of the tremor (200–400 ms) for the brain→contralateral hand direction with average values $\gamma_1 = 0.03$–0.05 and $\gamma_2 = 0.20$–0.25 (see footnote [4]).

[4]Figure 2 shows the longest tremor epoch. Unlike in fig. 2, in the averaged plots in fig. 3 the (significant) maximum of γ_1 differs from (the nonsignificant) $\gamma_1(0)$ within a confidence band. This is because the exact location of the maximum $\gamma_1(\Delta_1)$ varied in the range of 1–2 tremor periods between epochs. Such variations are due to fluctuations and are stronger for shorter epochs. Averaging over many (especially shorter) epochs decreases the maximum of γ_1 and, especially, broadens the confidence band.

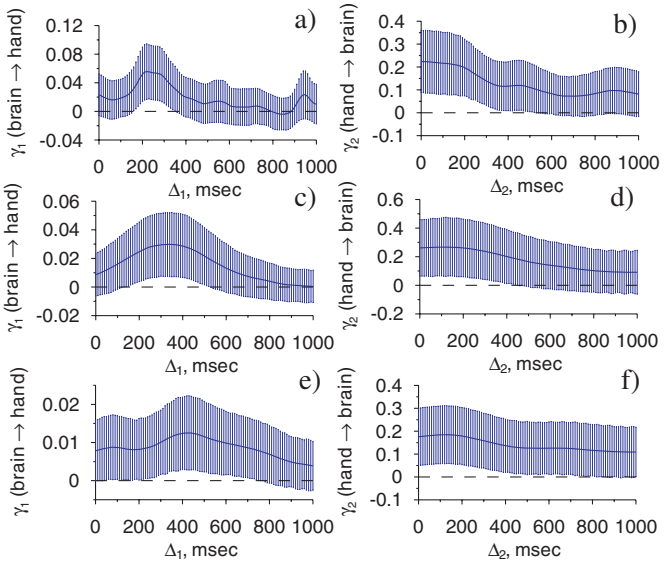

Fig. 3: Coupling characteristics obtained from the phase dynamics averaged over many epochs for each patient. Error bars indicate averaged values of the analytically estimated 95% confidence bands. a), b) Patient #1 (basic tremor frequency is 5 Hz, filter frequency band used to calculate the phases is 2–6 Hz, number of epochs is 14, duration of epochs ranges from 16.5 s to 83.5 s). c), d) Patient #2 (4 Hz, 2–6 Hz, 12, 17.5 s–45.0 s). e), f) Patient #3 (5 Hz, 3–7 Hz, 15, 15.0 s–55.0 s).

In all patients accelerometer signals were recorded bilaterally (from both hands) and LFPs only unilaterally. Patient # 2 had a unilateral tremor, contralateral to the implanted electrode. In contrast, patients #1 and 3 had a bilateral tremor, where the frequencies of left and right tremor were different, respectively. In patients #1 and 3 significant coupling between LFP and ipsilateral tremor was neither reliably and consistently detected with CCF nor with phase dynamics modelling.

Simple model simulations. – To check our analysis, we applied it to a simple system of a noisy van der Pol oscillator (accounting for the nonlinearity of the accelerometer signal) and a strongly dissipative linear oscillator, reproducing the noise levels σ_j^2 of the tremor ($\sigma_1^2 \approx 0.1$) and the LFP signal ($\sigma_2^2 \approx 1.0$), respectively. Accelerometer ($a_1 = \ddot{y}_1$) and LFP (y_2) model oscillators read

$$\ddot{y}_1(t) - (\lambda - y_1^2(t))\dot{y}_1(t) + y_1(t) = k_1(y_2(t-\tau_1) - y_1(t)) + \epsilon_1(t), \tag{2}$$

$$\ddot{y}_2(t) + 0.15\dot{y}_2(t) + y_2(t) = k_2(y_1(t-\tau_2) - y_2(t)) + \epsilon_2(t) \tag{3}$$

with independent white noises ϵ_1, ϵ_2 with $\langle \epsilon_k(t)\epsilon_k(t')\rangle = 0.01\delta(t-t')$, $\lambda = 0.05$. To generate time series, we integrated the equations with Euler technique and step size 0.01. Sampling interval was set equal to 0.15, *i.e.* approximately 40 data points per basic period of oscillations.

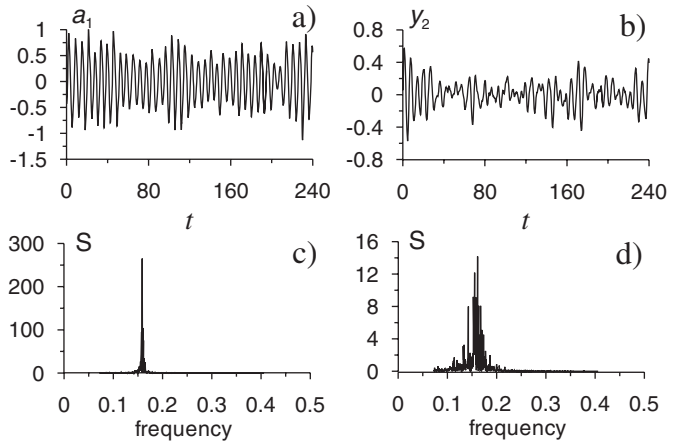

Fig. 4: A simulation of eqs. (2), (3) for $k_1 = k_2 = 0$. Time courses: a) ($a_1(t) = \ddot{y}_1(t)$), the analogue of the bandpass-filtered accelerometer signal $x_1(t)$ from fig. 1(e). b) $y_2(t)$, the analogue of the bandpass-filtered LFP $x_2(t)$ from fig. 1(f). t is the dimensionless time. c), d) Power spectra of $a_1(t)$ and $y_2(t)$, which hardly change for k_1, k_2 as in fig. 5.

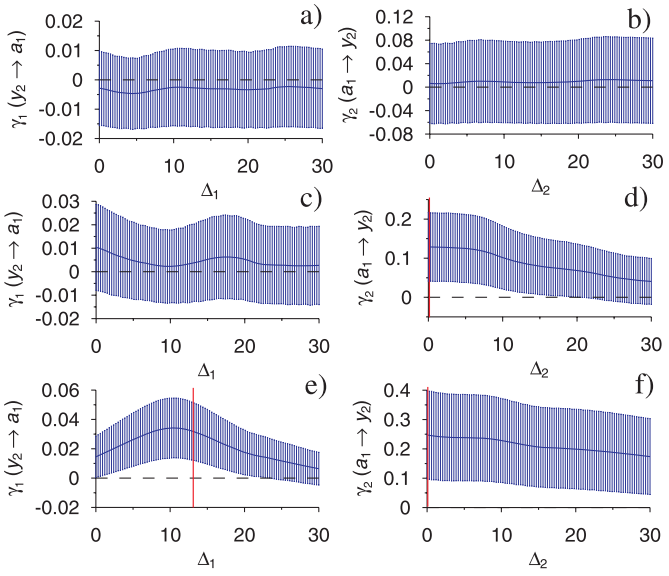

Fig. 5: Coupling characteristics obtained from the phase dynamics of the model (2) and (3), averaged over ensembles of time series. Error bars indicate averaged values of the analytically estimated 95% confidence bands. Vertical red lines indicate true delay times. a), b) Uncoupled oscillators. c), d) Unidirectional coupling, $k_1 = 0$, $k_2 = 0.07$, $\tau_2 = 0$. e), f) Bi-directional time-delayed coupling, $k_1 = 0.2$, $\tau_1 = 13.0$, $k_2 = 0.05$, $\tau_2 = 0$.

The reasoning behind our minimal model equations (2) and (3) is as follows. First, we chose a nonlinear oscillator (2) as a model of the accelerometer signal, since in a large number of tremor epochs our attempt to reconstruct a model equation from the accelerometer time series resulted in such a model (in preparation). In fact, due to its central pattern generators the spinal cord is able to produce self-sustained rhythmic neural and muscular activity [31]. Moreover, similar conclusions were previously obtained for both Parkinsonian and essential tremor dynamics [32]. Below, we report the results for a van der Pol oscillator which is close to the point of an Andronov-Hopf bifurcation and demonstrates self-sustained oscillations (positive value of λ) perturbed by noise. Note, we are not dependent on a deterministically self-sustained oscillation, since the results of the coupling estimation are very similar for small negative λ as well. The reason is that noise induces similar oscillations for small negative and small positive values of λ. Second, we chose a linear oscillator modelling the LFP signal, since the construction of polynomial autoregressive models with different polynomial orders does not exhibit pronounced nonlinearity (in preparation). Time series and power spectra estimates for the uncoupled oscillators (2) and (3) are shown in fig. 4 (cf. fig. 1(c)–(f)).

We analyzed ensembles of time series generated by eqs. (2) and (3) with exactly the same procedure as applied to our experimental data (see above). For our numerical simulations we used ensembles consisting of 100 time series of the length of 100 basic periods. The averaged results of our coupling estimation for the observables $a_1(t)$ and $y_2(t)$ are shown in fig. 5 in the same form as for the experimental results from fig. 3. Without coupling ($k_1 = k_2 = 0$), we obtained the results shown in fig. 5(a), (b). In particular, we obtained no false coupling detection on average. For unidirectional "tremor" $\rightarrow$ "brain" coupling ($k_1 = 0$, $k_2 = 0.07$, $\tau_2 = 0$), we observed the unidirectional coupling pattern, fig. 5(c), (d). The coupling pattern observed in fig. 3 is qualitatively reproduced in our model for bi-directional time-delayed coupling, *e.g.*, for $k_1 = 0.2$, $\tau_1 = 13.0$, $k_2 = 0.05$, $\tau_2 = 0$ (fig. 5(e), (f)). γ_1 gets maximal for $\Delta_1 = 10.7$ which is smaller than $\tau_1 = 13.0$ by 1/3 of the basic period. For a range of true coupling coefficients and time delay values, we observed that the time delay estimate is less than the true time delay by 1/4–1/2 of the basic period. Thus, with this simple example we illustrated that reasonable estimates of the delay times are obtained with our approach. However, our model simulations showed that time delay estimates may have an error of up to half a basic period, and, hence, the time delays are not determined very accurately. Yet, we can conclude that the time delay in the brain $\rightarrow$ tremor influence estimated from our experimental data is greater than the delay in the tremor $\rightarrow$ brain influence[5].

Conclusion. – Our results and previous studies [16,17,23,33] fit to the assumption that the subcortical oscillations drive and synchronize premotor and motor

[5] A comparison of the strength of the brain $\rightarrow$ tremor and tremor $\rightarrow$ brain influence is difficult, because the noise level σ_j^2 is greater for the LFP. Different normalizations yield different relative strengths: i) A direct comparison of γ_1 to γ_2 (see footnote [2]) yields that the tremor $\rightarrow$ brain influence is stronger. ii) Normalizing γ_k by the variance of the phase increments, we get an equalized bidirectional influence.

cortex (which activates the contralateral muscles via the spinal cord) [16,17,23,33]. But the long brain→tremor delay indicates a more complex mechanism compared to a simple forward transmission. In contrast, the short tremor→brain delay fits to a direct neural transmission time of a proprioceptive feedback loop (see [18]). Our results provide a new picture of the old servo loop oscillation concept, where feedback and feedforward are acting via straight transmission lines [15]. Rather, the synchronized subcortical oscillatory activity feeds into a multistage re-entrant processing network, most likely involving cortico-subcortical and spinal reflex loops (see [15–17]).

The subcortical oscillatory activity, measured as local field potential by depth electrodes, is generated by the synchronized current changes in a large number of neurons [34]. As shown here, the synchronized subcortical neural oscillation drives the peripheral tremor. Accordingly, the subcortical oscillation represents an ideal candidate for a therapeutic control intervention accomplished by desynchronization methods [35], such as coordinated reset stimulation [36]. Put otherwise, our results suggest to specifically counteract tremor generation by desynchronizing the abnormally synchronized subcortical population of oscillatory neurons, *e.g.*, in the classical targets STN and VIM. In contrast, as yet, permanent high-frequency deep brain stimulation is applied to suppress Parkinsonian symptoms [37]. This type of stimulation strongly alters the affected neuronal population, *e.g.*, by completely blocking the neuronal firing [38].

* * *

We thank M. Rosenblum and the referees for their comments. We thank the EU network of excellence BioSim (LSHB-CT-20004-005137) and the Russian Foundation for Basic Research (grant 07-02-00747).

REFERENCES

[1] Pikovsky A., Rosenblum M. and Kurths J., *Synchronization. A Universal Concept in Nonlinear Sciences* (Cambridge University Press, Cambridge) 2001; Kuramoto Y., *Chemical Oscillations, Waves and Turbulence* (Springer-Verlag, Berlin) 1984; Haken H., *Advanced Synergetics* (Springer, Berlin) 1983; Winfree A. T., *The Geometry of Biological Time* (Springer, Berlin) 1980.
[2] Rosenblum M. G. and Pikovsky A. S., *Phys. Rev. E*, **64** (2001) 045202.
[3] Cimponeriu L., Rosenblum M. and Pikovsky A., *Phys. Rev. E*, **70** (2004) 046213.
[4] Kralemann B. *et al.*, *Phys. Rev. E*, **76** (2007) 055201.
[5] Smirnov D. and Bezruchko B., *Phys. Rev. E*, **68** (2003) 046209.
[6] Mokhov I. I. and Smirnov D. A., *Geophys. Res. Lett.*, **33** (2006) L0378, doi:10.1029/2005GL024557.
[7] Smirnov D. A., Karpeev I. A. and Bezruchko B. P., *Sov. Tech. Phys. Lett.*, **33** (2007) 147.
[8] Feldmann U. and Bhattacharya J., *Int. J. Bifurcat. Chaos*, **14** (2004) 505.
[9] Marinazzo D., Pellicoro M. and Stramaglia S., *Phys. Rev. E*, **73** (2006) 066216.
[10] Hlavackova-Schindler K. *et al.*, *Phys. Rep.*, **441** (2007) 1.
[11] Palus M. and Vejmelka M., *Phys. Rev. E*, **75** (2007) 056211.
[12] Rosenblum M. G. *et al.*, *Phys. Rev. E*, **65** (2002) 041909; Palus M. and Stefanovska A., *Phys. Rev. E*, **67** (2003) 055201; Luchinsky D. G. *et al.*, *Phys. Rev. E*, **72** (2005) 021905.
[13] Llinas R. and Jahnsen H., *Nature*, **297** (1982) 406; Pare D., Curro'Dossi R. and Steriade M., *Neuroscience*, **217** (1990) 35; Lenz F. A. *et al.*, *Brain*, **117** (1994) 531.
[14] Nini A. *et al.*, *J. Neurophysiol.*, **74** (1995) 1800.
[15] Stilles R. and Pozos R., *J. Appl. Physiol.*, **40** (1976) 990.
[16] Rivlin-Etzion M. *et al.*, *Curr. Opin. Neurobiol.*, **16** (2006) 629.
[17] Brown P., *Mov. Disord.*, **18** (2003) 357.
[18] Eichler M., *Handbook of Time Series Analysis*, edited by Winterhalder M., Schelter B. and Timmer J. (Wiley-VCH, Berlin) 2006, p. 335.
[19] Wang S. *et al.*, *J. Franklin Inst.*, **344** (2007) 180.
[20] Smirnov D. and Andrzejak R., *Phys. Rev. E*, **71** (2005) 036207.
[21] Smirnov D. *et al.*, *Chaos*, **17** (2007) 013111.
[22] Treuer H. *et al.*, *Radiother. Oncol.*, **77** (2005) 202.
[23] Tass P. A. *et al.*, *Phys. Rev. Lett.*, **81** (1998) 3291.
[24] Rybski D., Havlin S. and Bunde A., *Physica A*, **320** (2003) 601.
[25] Gozolchiani A. *et al.*, *Physica A*, **366** (2006) 552.
[26] Bartsch R. *et al.*, *Physica A*, **383** (2007) 455.
[27] Gabor D., *J. IEEE London*, **93** (1946) 429.
[28] Granger C. W. J., *Econometrica*, **37** (1969) 424.
[29] Schreiber T. and Schmitz A., *Physica D*, **142** (2000) 346.
[30] Dolan K. and Neiman A., *Phys. Rev. E*, **65** (2002) 026108.
[31] Dietz V., *Clin. Neurophysiol.*, **114** (2003) 1379.
[32] Timmer J. *et al.*, *Chaos*, **10** (2000) 278.
[33] Timmermann L. *et al.*, *Brain*, **126** (2003) 199.
[34] Brown P. and Williams D., *Clin. Neurophysiol.*, **116** (2005) 2510.
[35] Tass P. A., *Phase resetting in medicine and biology: Stochastic modelling and data analysis* (Springer Verlag, Berlin) 1999; *Europhys. Lett.*, **53** (2001) 15; Tass P. A., Hauptmann C. and Popovych O. V., *Int. J. Bifurcat. Chaos*, **16** (2006) 1889.
[36] Tass P. A., *Biol. Cybern.*, **89** (2003) 81.
[37] Benabid A. L. *et al.*, *Lancet*, **337** (1991) 403.
[38] Benabid A. L., Benazzous A. and Pollak P., *Mov. Disord.*, **17** (2002) 73.